

Article

Looking Like Gold: Chlorite and Talc Transformation in the Golden Slip Ware Production (Swat Valley, North-Western Pakistan)

Lara Maritan ^{1,*}, Rebecca Piovesan ², Maria Chiara Dalconi ¹, Jordi Rius ³, Anna Crespi ³, Oriol Vallcorba ⁴ , Lluís Casas ⁵ , Massimo Vidale ⁶ and Luca Maria Olivieri ⁷

¹ Department of Geosciences, University of Padova, Via Gradenigo 6, 35131 Padova, Italy; mariachiara.dalconi@unipd.it

² Piovesan Consulting, Via Venozzi, 28/E, 31040 Volpago del Montello, Italy; rebecca.piovesan@gmail.com

³ Institut de Ciència de Materials de Barcelona (ICMAB), Campus de la UAB, 08193 Bellaterra, Catalonia, Spain; jordi.rius@icmab.es (J.R.); acrespi@icmab.es (A.C.)

⁴ ALBA Synchrotron Light Facility, Carrer de la Llum 2-26, 08290 Cerdanyola del Vallès, Barcelona, Catalonia, Spain; ovalcorba@cells.es

⁵ Departament de Geologia, Universitat Autònoma de Barcelona, 08193 Bellaterra, Catalonia, Spain; Lluís.Casas@uab.cat

⁶ Department of Cultural Heritage: Archaeology and History of Art, Cinema and Music, University of Padova, Piazza Capitaniato 7, 35139 Padova, Italy; massimo.vidale@unipd.it

⁷ ISMEO Italian Archaeological Mission in Pakistan, 31-32 College Colony, 19200 Saidu Sharif (Swat), Pakistan; act.fieldschool@gmail.com

* Correspondence: lara.maritan@unipd.it; Tel.: +39-049-8279143

Received: 19 April 2018; Accepted: 5 May 2018; Published: 8 May 2018



Abstract: The archaeometric study of the “golden slip” ware (second century BCE—fourth century CE) at the site of Barikot (Swat, north-western Pakistan) aimed to define its manufacturing technology and provenance of the raw materials used. For this reason, a multianalytical approach consisting of the microscopic, microstructural and mineralogical analysis of both the golden slip and the ceramic paste was adopted. The slip was found to be composed by platy minerals, microchemically identified as talc and chlorite; their intimate association indicated clearly that they derived from a chlorite-talc schist. This rock is geologically available near the site in the “green stones” lenses within the Mingora ophiolites outcropping in the Swat valley. Due to the use of this stone also for the production of stone tools, it cannot be excluded that the chlorite-talc schist used for the golden slip can be derived from manufacturing residues of the Gandharan sculptures. In order to constrain the firing production technology, laboratory replicas were produced using a locally collected clay and coating them with ground chlorite-talc schist. On the basis of the mineralogical association observed in both the slip and the ceramic paste and the thermodynamic stability of the pristine mineral phases, the golden slip pottery underwent firing under oxidising conditions in the temperature interval between 800 °C and 850 °C. The golden and shining looks of the slip were here interpreted as the result of the combined light reflectance of the platy structure of the talc-based coating and the uniform, bright red colour of the oxidized ceramic background.

Keywords: talc; chlorite; enstatite; microstructure; mineralogy; synchrotron through-the-substrate microdiffraction; experimental replicas

1. Introduction

Ancient ceramic vessels have always been decorated with different techniques [1], with their decorations, in many cases, being the most visible and accessible attributes, in addition to the shape, on

the basis of which a ceramic can be typologically [2] and culturally classified. Among others, ceramic specialists refer with the term slip (engobe) to be clay-based coatings generally characterised by a different colour than the ceramic paste. These coatings also provide, when high firing temperature promotes the partial melting of their clay minerals, a waterproof character to the treated surfaces. The study of slips also using different methodological analytical approaches can provide information on their production technology [3–6], allowing to better constrain their ceramic class.

Very interestingly, within the occupation levels at the ancient urban site of Barikot (Swat, north-western Pakistan) a peculiar pottery class was discovered; the so-called golden slip ware is characterised by the presence of a slip with a bright-gold colour and a pearly, very vitreous lustre on the external surface and sometimes also on the internal one (Figure 1). This type of slip was used to coat generally small-sized carinated or bi-carinated jars characterised by restricted mouths, everted flat rims and discoidal flat non-contiguous bases. In some cases, the golden slip was completed with red decorations and the corresponding ceramic class defined as red-on-golden slip ware.

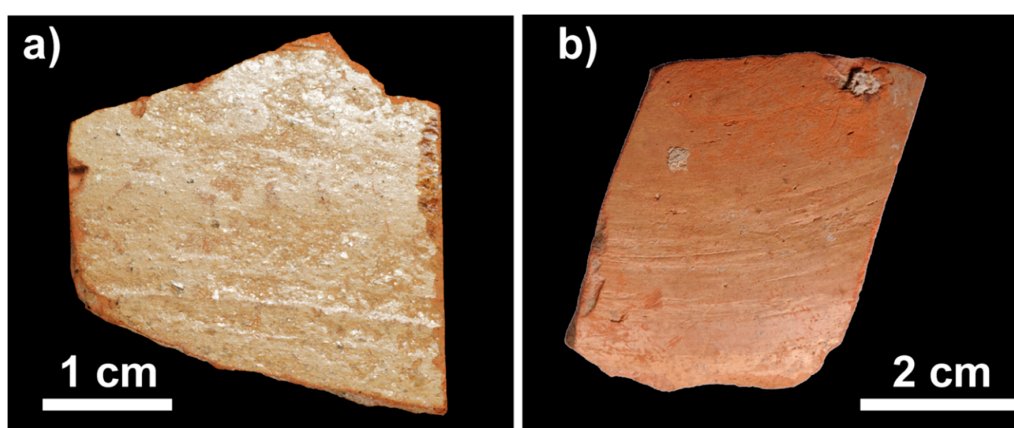


Figure 1. Photographs of golden slip ware from Barikot: (a) Fragment with a beautiful and almost perfectly preserved golden slip (sample BKG 11 K-103 1372); (b) Fragment in which the slip is thinner, partially eroded and looks less shiny (sample BKG 11 B-13 1078).

The golden slip ware, despite being a sporadic finding, was attested in various occupation levels at Barikot [7–10], covering quite a wide time span from the Indo-Greek/Hellenistic acculturation phase to the Late Kushan/Kushana-Sasanian phase, from the second century BCE to the fourth century CE (Table 1).

The inscribed (non-carinated) pots found at other sites of Gandhāra (the ancient region between the modern-day northern Pakistan and Afghanistan) are possibly also associated with this type of slips. These show a “light wash of slip, of cream or buff color” [11], which may correspond to the “golden” slip as is presented here.

This gold-like slip was used to make the vessels precious; hence, it inspired the present archaeometric studies, aimed at the definition of its manufacturing technology with particular interest in the firing conditions as well as the mineralogical nature and provenance of the raw materials used. For this reason, a set of golden slip sherds from Barikot were analysed with different minero-petrographic methods and compared with replicas obtained in the laboratory using the same raw materials adopted in ancient times, as identified from the analytical study.

2. Materials and Methods

A set of six samples were selected from the continuous stratigraphic sequence of Barikot (Table 1) and analysed according to a multianalytical approach consisting in the microstructural, mineralogical and chemical analysis of both the slip and the ceramic body.

Specifically, thin sections of potsherds were observed under the polarized-light microscope to perform a petrographic description of the slip and that of the ceramic body, following the description procedure and terminology proposed by Whitbread [12,13] and revised by Quinn [14]. Microstructural analysis was performed by a scanning electron microscope (SEM) using a CamScan MX 2500 coupled to an EDS spectrometer equipped with a LaB₆ cathode (Ted Pella Inc., Redding, CA, USA) and operating at an electric potential difference of 20 kV, with a current of 160 nA, with a working distance of about 20 mm. Mineralogical analysis was performed by X-ray powder diffraction (XRPD) on the samples (both ceramic body and slips mechanically separated from the body), finely grounded in a agate mortar, using a PANalytical X'Pert PRO diffractometer in Bragg–Brentano geometry, equipped with a Co X-ray tube (40 kV and 40 mA, Co-K α radiation) and a X'Celerator detector (PANalytical, Almelo, The Netherlands). Diffractograms were acquired in the 3°–85° 2 θ range, with a step size of 0.017° and a counting time of 1 s per step. Due to the very thin slip applied on the pottery, only for some samples it was possible to separate mechanically enough slip powder from the ceramic body to be analysed by XRPD. X-ray diffraction patterns allowed mineralogical composition to be retrieved for both slip and ceramic bodies using PANalytical HighscorePlus software (Version 4.7, Panalytical B.V., Almelo, The Netherlands).

Table 1. List of the analysed golden slip ware potsherds with the indication of the archaeological level from which they are from, the age, the composition of the slip and of the ceramic body as observed microscopically, by X-ray powder diffraction (XRPD) (between brackets) and synchrotron μ XRD (between brackets, in *italic*), and at the μ -Raman [between square brackets]. Estimated firing temperatures, constrained on the basis of the mineralogical composition of the ceramic body and the slip, are also reported. Abbreviations: Amp: amphibole; Carb: carbon; En: enstatite; Fds: feldspars; Fo: forsterite; Hem: hematite; Ill/Ms: illite/muscovite; Qz: quartz; Tlc: talc. Macro-phases: VIII/5b: end third century–beginning fourth century CE; VI/4b: end first–beginning second century CE; III/3a: middle second century BCE; III/3a: c. 369–106 BCE 100% 2 σ .

Sample	Macrophase (Chronology)	Slip	Ceramic Body Paste
BKG 11 B-13-1078	VIII/5b	chlorite-talc schist * (Tlc, Qz, Ill/Ms, Amp) (<i>Tlc</i>) [Tlc, Carb] 800–850 °C	amphibolite-rich (Qz, Fds, Ill/Ms, Amp, Hem) 750–900 °C
BKG 11 K-105-1372	VI/4b	chlorite-talc schist * (Tlc, En, Qz, Amp, Fds) (<i>Tlc, En, Fo</i>) [Tlc, Carb] 800–850 °C	amphibolite-rich (Qz, Amp, Fds, Ill/Ms) 750–900 °C
BKG 11 K-105-1373		chlorite-talc schist * (Ill/Ms, Qz, Fds) (<i>Ill/Ms</i>) [Carb, Ms] 850–900 °C	quartzite-rich (Qz, Fds, Ill/Ms) 750–900 °C
BKG 11 K-105-1663	III/3a	chlorite-talc schist * (Qz, Fds) (<i>En, Fo</i>) [Carb, En] >900 °C	fine (Qz, Fds, Hem) >900 °C
BKG 11 K-105-1673	III/3a	chlorite-talc schist * [Carb, He] 800–850 °C	fine (Qz, Fds, Ill/Ms, Amp, Hem) 750–950 °C
BKG 11 K-105-1687	<u>III/3a</u>	chlorite-talc schist * (Tlc, Qz, Fds, Ill/Ms, Amp, Hem) [Tlc, Car] 800–850 °C	fine (Qz, Fds, Ill/Ms, Amp, Hem) 750–950 °C

* Referable to the pre-firing material.

Moreover, the slip of some of the potsherds (sample: BKG 11 B-13-1078, BKG 11 K-105-1372, BKG 11 K-105-1373, BKG 11 K-105-1663) were also analysed by synchrotron through-the-substrate microdiffraction (synchrotron tts- μ XRD) at the Material Science and Powder Diffraction beamline [15] from ALBA synchrotron facility (Cerdanyola del Vallès, Barcelona, Spain), using a focused spot size of $15\text{ }\mu\text{m} \times 15\text{ }\mu\text{m}$ (FWHM) horizontal \times vertical, and a photon energy of 29.2 keV. The synchrotron tts- μ XRD allows collection of data directly on the thin sections preserving the textural context and allowing local mineral phase identification and/or structure determination [16–18]. Mineralogical composition was retrieved for the analysed areas using Sleve+ plugin within PDF4+ database (ICDD, International Centre for Diffraction Data, Newtown Square, PA, USA). Slips were also analysed by micro-Raman using a DXR Thermo Scientific Raman microscope (Thermo Fisher Scientific, Waltham, MA, USA), equipped with a frequency-stabilized single mode diode 532 nm depolarised laser. Spectra were acquired directly from the potsherd slipped surface, using a laser power of 8 mW, spectrograph aperture of 25–50 μm pinhole and using a 50X low distance objective, therefore with a spectral resolution in the range $2.7\text{--}4.2\text{ cm}^{-1}$ and a spatial resolution of $1.1\text{ }\mu\text{m}$.

In order to properly define the production technology of the golden slip, a series of replicas were produced using a clay collected from the alluvial deposits of the Swat river near Barikot. On the formed and dried briquettes, the slip was applied following two different approaches: (i) immersing the briquettes into a barbotine of finely ground chlorite-talc schist; (ii) drawing the surface with a brush immersed into the barbotine. The briquettes were then fired into a laboratory MT furnace equipped with a digital microprocessor (Digitronik DCP200, Yamateke-Honeywell, Azbil Corporation, Tokyo, Japan) for firing curve control, according to kiln-like conditions [19] that corresponded probably to those originally adopted at Barikot. Kiln-firing conditions are generally characterised by a low heating rate (a few hundreds of degrees per hour), long residence time (many hours), and redox conditions may vary depending on the type of kiln, although they are generally oxidising [1,20]. Briquettes were fired between $750\text{ }^{\circ}\text{C}$ and $950\text{ }^{\circ}\text{C}$, every $50\text{ }^{\circ}\text{C}$, in an oxidising atmosphere (in air with a $f(\text{O}_2) \sim 0.2$ bars), at a heating rate of $200\text{ }^{\circ}\text{C/h}$, residence time of 6 h, and cooling rate of about $50\text{ }^{\circ}\text{C/h}$. The firing interval was chosen on the basis of the thermal stability of the mineral phases observed in the golden slip analysed from the archaeological potsherds. In addition to the briquettes, a finely ground powder of chlorite-talc schist was fired in the same conditions to define the mineralogical evolution during firing of this material. After firing, the powder was analysed by XRPD using the same instrumental conditions described above and compared with that of the potsherd. The slip of the fired briquettes was also analysed by micro-Raman.

3. Results and Discussion

3.1. The Ceramic Body

The analysis of the ceramic body shows that different types of paste were used to produce the golden slip ware:

- fine paste: in which inclusions are scarce, with a c:f (coarse:fine) ratio of 20:80, mainly composed by silt-sized angular crystals of quartz, associated to rare plagioclase, opaque minerals and mica flakes (muscovite and biotite), and fine sand-sized fragments of rounded quartzite (Figure 2a), embedded into an optically active micromass with a speckled b-fabric (birefringent fabric); scarce pores as vughs and channels occur in the groundmass;
- quartzite-rich paste: with inclusions with a c:f ratio of about 40:60, showing a bi-modal grain-size distribution, with silt-sized fraction composed predominantly by quartz associated to scarce plagioclase, opaque minerals and white and brown micas, showing a grain-size gap with the coarse sand-sized fragments of quartzite (Figure 2b); the groundmass is characterised by a higher porosity, with vughs and channels reaching larger size than in the fine paste;
- amphibolite-rich paste: characterised by abundant inclusions (c:f ratio of about 40:60), with a bimodal grain-size distribution, in which silty and fine sand-sized grains predominantly of quartz

and associated plagioclase, opaque minerals and micas flakes showing a grain-size gap with the sand-sized fragments of amphibolite (Figure 2c); also in this case the porosity is higher and reaches larger size than in the fine paste.

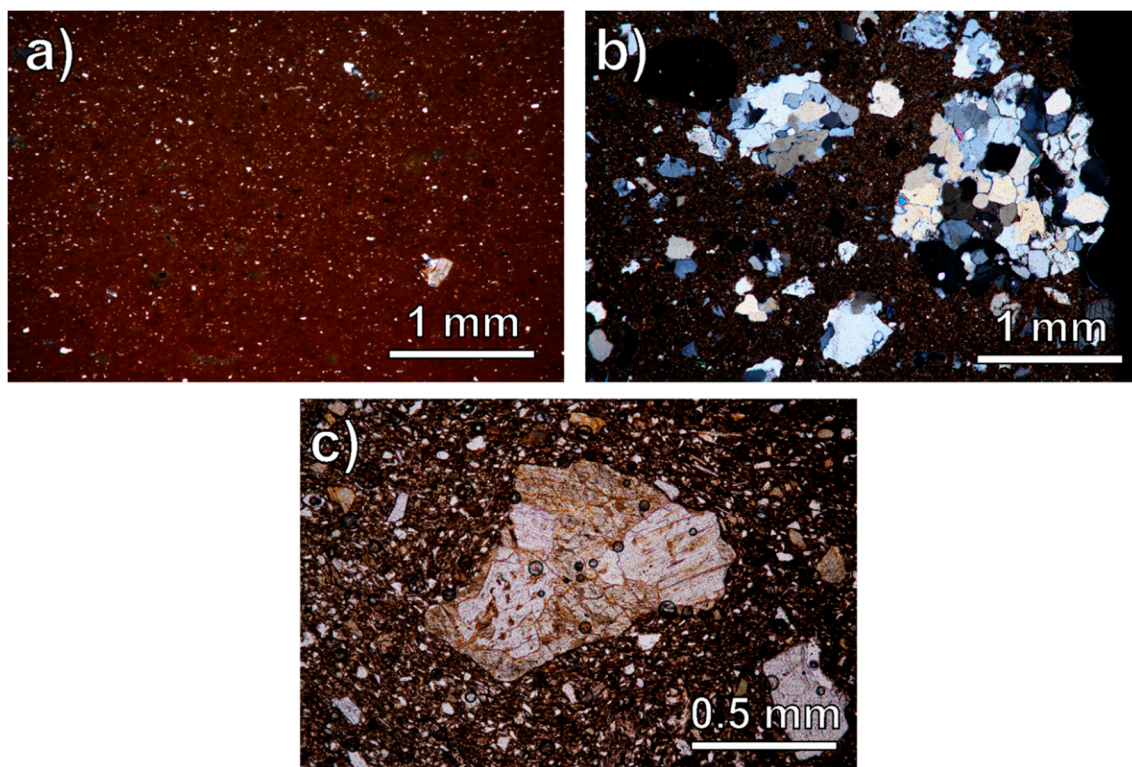


Figure 2. Photomicrographs of the ceramic pastes of the golden slip ware under polarised-light microscope: (a) Fine paste (sample BKG 11 B-13 (1078); crossed-polarised light); (b) Quartzite-rich paste (sample BKG 11 K-105-1373, crossed-polarised light); (c) Amphibolite-rich paste (sample BKG 11 K-103-1372, crossed-polarised light).

These ceramic pastes were, therefore, produced according to different recipes. In particular, while the first described was made using just a silt-clayey material, probably as collected from the fine alluvial deposits of the Swat river, the latter two were produced adding a sieved sand-size temper, as attested by the well-sorted size of the large inclusions. In relation to the provenance, the petrographic nature of the inclusions is consistent with the geology of the area, and specifically, while the amphibolite outcrops in the Kohistan Island Arc just north of Barikot, the quartzite could come from the Swat–Buner schists of the Indo–Pakistan Plate outcropping east and south of Barikot (Figure 3). Therefore, these tempers were probably collected in the sand alluvial sediments of the Swat river and the different composition observed in the potsherds is probably related to the different points of collection of the sand sediment, in any case possibly near the site of Barikot.

The mineralogical composition of the ceramic body (Table 1) vary from paste to paste, but in all the cases quartz, feldspars and illite/muscovite are present, often associated to hematite and amphibole. The occurrence of hematite is consistent also with the colour of the ceramic body which is for all the studied potsherds uniform in sections with reddish hues. Moreover, since the pottery was locally produced, the lack of kaolinite, chlorite and smectite (constituting with illite/muscovite, quartz, feldspar and amphibole the raw clay material from the Swat valley as sampled near the site) indicates that the pottery was fired at a temperature exceeding 750 °C and below 900 °C. Kaolinite, in fact, decomposes at temperatures around 550 °C [21,22], chlorite and smectite at temperatures around

750 °C, whereas hematite nucleates at temperatures higher than 750 °C [23], and illite/muscovite persists until around 900–950 °C [19,24].

Only in one sample (BKG 11 K-105-1663) illite/muscovite was not detected, indicating a firing temperature exceeding 900 °C.

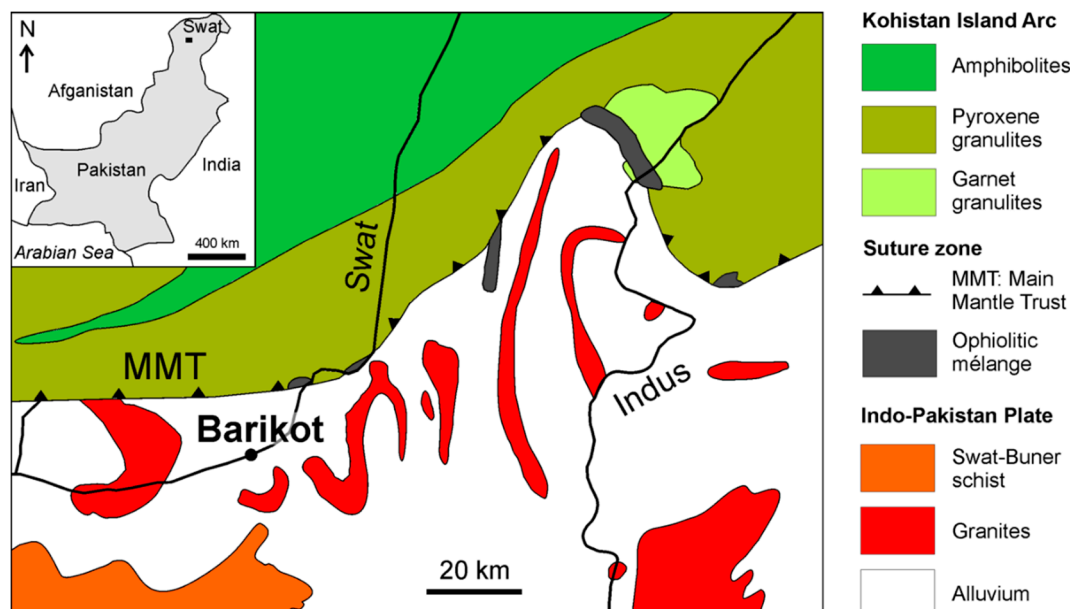


Figure 3. Geological sketch of the Swat valley near Barikot (modified from Faccenna et al. [25]).

3.2. The Slip

Macroscopically, the analysed potsherds presented only in one case (sample BKG K-103-1372) a very well-preserved golden slip (Figure 1a), whereas in the others, both the external and internal pottery surfaces were partially eroded and the slip had detached from the ceramic body, so that it is preserved only in small portions or as thin layers which can be barely seen (Figure 1b).

Microstructurally, the slip is characterised by a variable thickness among the studied samples, varying between 20 and 50 µm (Figure 4a,b), and it is formed by flakes, arranged parallel to the ceramic body, showing a clear cleavage and belonging to two different phases, as can be seen from the different grey colour in the backscattered electron image in the SEM (Figure 4). The microchemical composition of these phases corresponds to that of talc and chlorite, respectively. More in detail, the high magnesium content of chlorite, despite semi-quantitatively measured at the EDS, indicates that this phase can be defined as a clinocllore (with $Fe/(Fe + Mg) = 0.175$) or a talc-chlorite ($Fe_{tot} = 1.5$; $Si = 7.84$), according to Bayley [26] and Hey [27], respectively. Talc and chlorite are in some cases also intimately associated within the same flake (Figure 4c), indicating that they derive from the same rock, and occasionally exhibit plastic deformation, with folded structures (Figure 4b), suggesting that the slip was obtained from a ground chlorite-talc schist.

The comparison with the talc schists collected from the gravel deposits of Swat river near Barikot shows that this rock, characterised by a schistose structure with thin levels of chlorite (about 20–30 µm thick) interbedded within the talc flakes (Figure 5), represents the material used to produce the powder that was then applied on the green body to produce the golden slip ware.

A detailed observation of the flakes forming the golden slip, shows that while talc flakes are characterised by a compact structure, chlorite lamellae often show small rounded pores and marked cleavage plains (Figure 4d). This microstructure, and in particular the occurrence of small pores, is compatible with hydroxyl degassing after chlorite decomposition. These portions, therefore, represent pseudomorph after chlorite.

This result is also supported by the optical microscopy analysis, for which, the slip appears under the parallel-polarised light with alternating elongated flakes showing a perfect cleavage, colour-less or light brown (Figure 6a), and interference colours (crossed-polarised light) of the third order for the former and brown for the latter (Figure 6b). It is clear that, while talc crystals preserved their original optical features, those of chlorite underwent changes during firing [28]. In fact, this mineral phase should exhibit a light green colour in parallel-polarised light and anomalous interference colour (generally purple or blue), while in the studied samples these are in both cases completely obliterated.

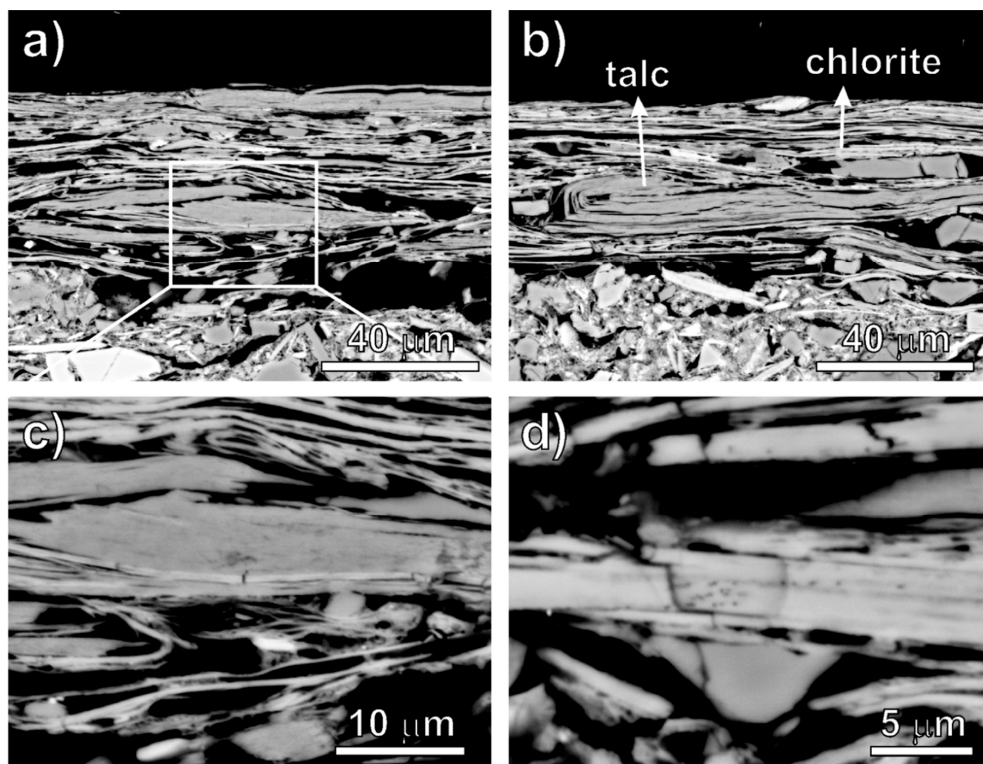


Figure 4. SEM-BSE images of the slip as observed from the archaeological sherds: (a) Alternating flakes of talc (dark grey) and pseudomorph after chlorite (light grey); (b) Folded flakes of talc embedded in the slip; (c) Intimate association of talc and pseudomorph after chlorite within the same flake; (d) Pseudomorph after chlorite flakes with degassing bubbles and marked cleavage plains.

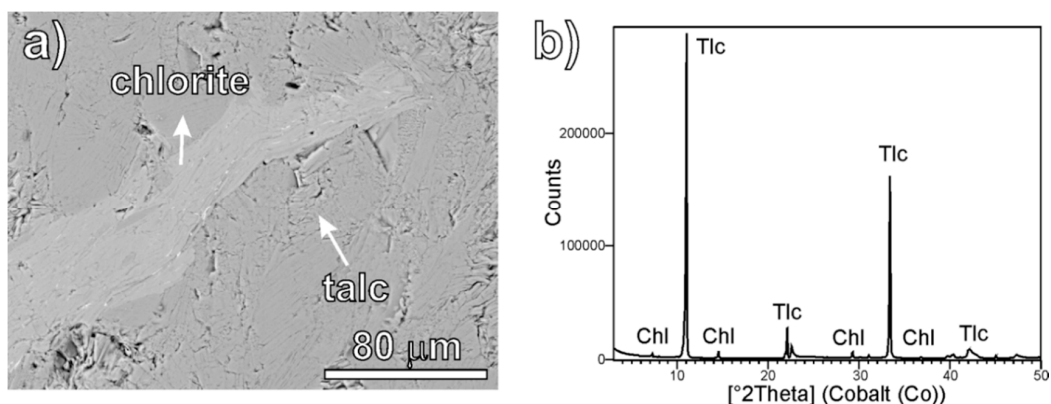


Figure 5. (a) SEM-BSE image; (b) XRPD pattern of the chlorite-talc schist collected from the coarse deposits on the Swat river near Barikot. Abbreviation as in caption of Table 1.

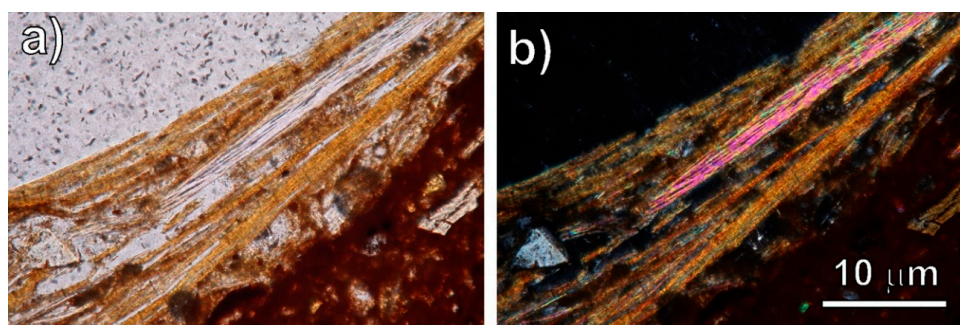


Figure 6. Photomicrographs of the slip of the potsherd BKG K-103-1372 under polarised-light microscope: (a) Parallel-polarised light; (b) Crossed-polarised light.

Most of the the slips mechanically separated from the ceramic bodies are mineralogically formed of talc and enstatite (Figure 7a) and no traces of chlorite are present in the diffraction patterns (Table 1). The occurrence of quartz, illite/muscovite, amphibole and feldspar are related to the ceramic body, which was also partially scratched when separating the slip. But, in some cases (BKG 11 K-105-1373, BKG 11 K-105-1663), no traces of talc were observed in the slip.

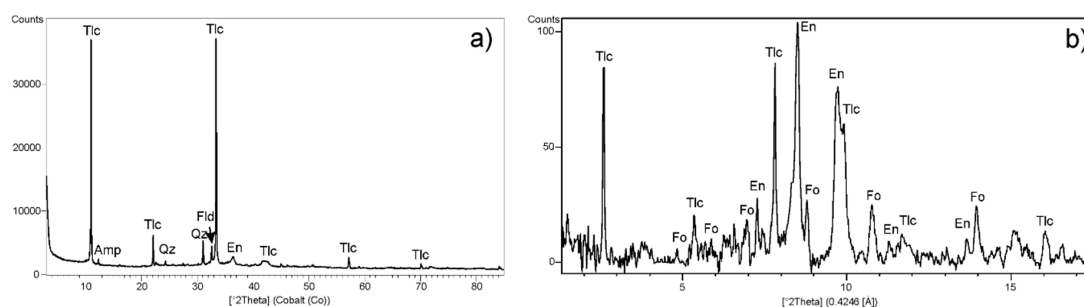


Figure 7. Diffraction pattern of the slip of potsherd BKG K-103-1372 as obtained by: (a) XRPD on the slip mechanically separated from the ceramic body; (b) Synchrotron tts-μXRD on areal analysis of the slip thin section. Abbreviation as in caption of Table 1.

The mineralogical composition of the slips analysed by synchrotron tts-μXRD is consistent with that observed in the mechanically separated slips (Table 1): they are formed of talc and contain small amounts of enstatite, whereas chlorite lacks that. Moreover, the occurrence of forsterite was also observed (Figure 7b), only on the basis of some of its peaks and not on their relative intensities. It is worth noting that intensity ratios observed by synchrotron tts-μXRD are not expected to necessarily follow those of a randomly oriented powder because the analysis is performed on a small area of the thin section. The use of scans rotating the sample around the Φ angle contributes in part to solve the situation. The newly formed phases, such as enstatite and forsterite are almost randomly distributed since they are cryptocrystalline (probably nano-sized), and no preferential orientation was observed in their case. The lack of forsterite in the XRPD pattern of the mechanically separated slips, is probably related to the small quantity of this phase and to the dilution effect of talc. The possibility, revealed using synchrotron tts-μXRD, of performing numerous analyses on small areas (of $15 \times 15 \mu\text{m}$) allowed to measure the diffraction patterns not on the bulk (typical of the XRPD) but on single flacks or some flacks (also partially decomposed and transformed). When the beam crossed pristine chlorite, the association enstatite and forsterite was, therefore, clearly observed, indicating the actual presence of altered pseudomorphs.

Enstatite represents the transformation product of talc [29] and indicates that talc partially decomposed. It also derives from the breakdown of Mg-rich chlorite, according to the reaction ($\text{chlorite} \rightarrow \text{enstatite} + \text{forsterite} + \text{spinel} + \text{H}_2\text{O}$), which is reported to take place at high pressure

(3 kbar) in deep geological environments [30]. In this case, despite the firing process that occurred on a superficial environment characterised by low pressure (1 bar = 10^{-3} kbar), both the pyroxene (enstatite) and olivine (forsterite) formed. Due to the reaction kinetics and to the short duration of the firing process compared to the geological process, only part of the pristine chlorite transformed into these newly formed mineral phases, while the rest formed an amorphous phase.

The micro-Raman analysis on the slip indicates that, in addition to the mineral phases observed by XRPD and by synchrotron μ XRD, small carbon particles are also present. These were laid down on the slip surface by the smokes circulating in the firing chamber and would derive from wood combustion. The peak height ratio (H_D/H_G) of the D (defect band, at 1350 cm^{-1}) and G (graphite band, at about 1580 cm^{-1}) bands of the carbon particles observed on the golden slip (Table 1), ranges within a wide interval (H_D/H_G : 0.75–0.98) also when various carbon particles are measured from the same sample. On the basis of the results of the recent experimental work of Deldicque et al. [31], the H_D/H_G values indicate different combustion temperatures, also within the same sample, in the interval between $800\text{ }^\circ\text{C}$ and about $1300\text{ }^\circ\text{C}$. It is worth noting that these temperatures have to be referred not to the firing chamber but to the temperature reached in the combustion chamber in different moments of the firing process: therefore, they record the gradual increase of the combustion temperature during the firing and are not indicative of the firing temperatures.

3.3. Firing Experiments

On the basis of the macroscopic aspect, the gold-like aspect was obtained only for briquettes fired at temperatures between $750\text{ }^\circ\text{C}$ and $850\text{ }^\circ\text{C}$. Moreover, slips obtained immersing the dried briquettes into a barbotine of finely ground chlorite-talc schist adhered better to the ceramic body, than those applied brushing the surface which were dustier.

The mineralogical evolution of the fired chlorite-talc schist clearly shows that the intensity of talc basal peaks progressively decreases until $900\text{ }^\circ\text{C}$, temperature at which they are very low (Figure 8). From $800\text{ }^\circ\text{C}$, enstatite peaks appear and progressively increase after the decomposition of talc (Ewel et al., 1935). Moreover, the background grows around $30^\circ 2\theta$, as a consequence of the gradual increase in amorphous phase related to the talc decomposition. Enstatite formed after the chlorite breakdown (at temperature lower than $750\text{ }^\circ\text{C}$), cannot be observed in the diffraction pattern of the firing experiment at $750\text{ }^\circ\text{C}$ (Figure 8), since it is under the XRPD detection limit. This is due to a dilution effect since chlorite is present in a very small quantity in the chlorite-talc schist.

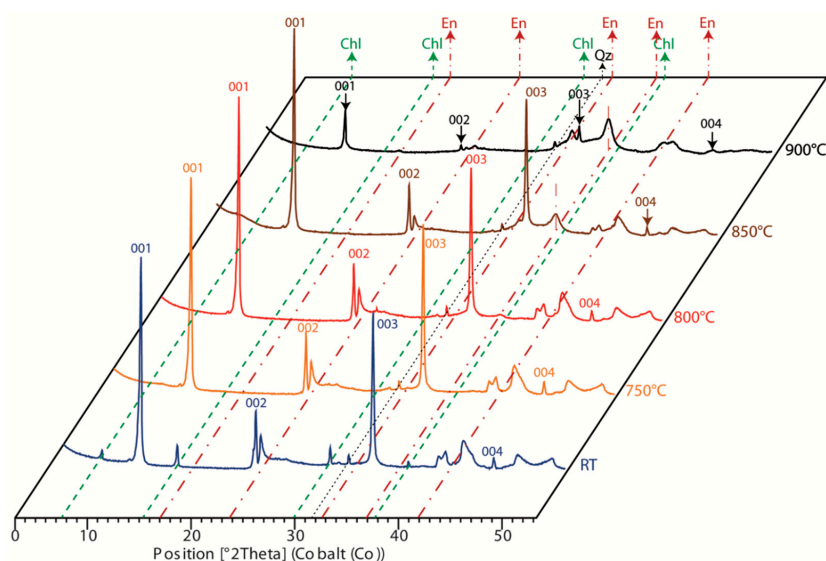


Figure 8. Diffraction patterns of the chlorite-talc schist at room temperature (RT) and fired between $750\text{ }^\circ\text{C}$ and $900\text{ }^\circ\text{C}$. Abbreviations as in caption of Table 1. (hkl) of talc peaks are also reported.

4. Conclusions

The petrographic, mineralogical and microstructural analysis of the golden slip ware, despite being performed on quite a restricted number of samples because of the archaeological rare availability, pointed out an interesting picture on the production technology of this ceramic class. When the paste type is considered in chronological terms, it can be observed that the golden slip ware in the earliest phases (third-second century BCE) was produced using a fine, probably also partially depurated paste, whereas in the most recent periods (first-third/early fourth century CE) it was manufactured using coarse tempered pastes (Table 1), indicating a clear change in the production recipes. While the recipe to produce the ceramic body changed over time, that of the golden slip was maintained, probably because it was the only way to obtain such peculiar and characteristic metallic-like aspects. Therefore, the gold-like aspect of the slip of this ceramic class is attributable to the combined effect of the pearly luster of talc on the red colour underneath ceramic body. The different luster of the analysed samples (Figure 1) can be related to both the different thickness of the slip, but also to the different firing temperature reached by each pot which, therefore, allowed the preservation of the talc crystalline structure or determined their breakdown. The comparison of the diffraction pattern of the slips mechanically separated (Figure 7) and the information obtained from the punctual analysis at the synchrotron μ XRD with the results of the firing experiments on the chlorite-talc schist, indicates that most of the potsherds were fired between 800 and 850 °C (Table 1), with some cases exceeding this temperature interval.

Talc schist was a rock locally available in the area of Barikot, since it occurs in the ophiolite outcrops of this region (Figure 3) and in the coarse alluvial deposits of the Swat river. The same type of rock was also used to produce Gandharan sculptures. Therefore, it is possible that the material used to produce the golden slip could derive from residues of this artisan activity. From a cognitive viewpoint, this technique represents a late development of the handed down acquaintance of the craftspeople of the Subcontinent with the pyrotechnological transformations of talc and steatite.

Author Contributions: L.M. planned the research. L.M. and M.C.D. conceived, designed and executed the firing experiments. L.M., M.C.D., R.P., A.C., L.C., J.R., O.V. carried out the analysis and interpreted the data. L.M.O. excavated the site, selected the archaeological materials, and provided the geological raw materials used to make the replicas. M.V. took the charge of controlling the archaeological metadata both in Pakistan and during the analytical process in Italy.

Acknowledgments: The authors thank the Directorate of Archaeology and Museums, Province of Khyber-Pakhtunkhwa (Pakistan), and the Department of Archaeology and Museums, Government of Pakistan for granting respectively the export permit and license for destructive analysis. The part of the research made in Pakistan was possible thanks to the support of the ISMEO Italian Archaeological Mission/ACT-Field School project. This research was possible thanks to the financial support of University of Padova (project: BIRD160990/16), Spanish Ministerio de Economía y Competitividad (project: CGL2013-42167-P), MINECO/FEDER (project MAT2015-67953-P) and the synchrotron facilities (experiment AV-2017022081). The authors are grateful to anonymous referees for their constructive review of this manuscript.

Conflicts of Interest: The authors declare no conflict of interest.

References

1. Rye, O. *Pottery Technology: Principles and Reconstruction*; Taraxacum Inc.: Washington, DC, USA, 1981; ISBN 978-0960282227.
2. Santacreu, A.D.; Trias, C.M.; Rosselló, G.J. Formal Analysis and Typological Classification in the Study of Ancient Pottery. In *The Oxford Handbook of Archaeological Ceramic Analysis*; Oxford Handbooks in Archaeology; Oxford, UK, 2016; ISBN 978-0199681532.
3. Schreiber, T. *Athenian Vase Construction—A Potter's Analysis*; The J. Paul Getty Museum: Malibu, CA, USA, 1999; ISBN 978-0892364664.
4. Mirguet, C.; Dejoie, C.; Roucau, C.; De Parseval, P.; Teat, S.J.; Sciau, P. Nature and Microstructure of Gallic Imitations of Sigillata Slips from the La Graufesenque Workshop. *Archaeometry* **2009**, *51*, 748–762. [[CrossRef](#)]
5. Leon, Y.; Sciau, P.; Goudeau, P.; Tamura, N.; Webb, S.; Mehta, A. The Nature of Marbled Terra Sigillata Slips: A Combined μ XRF and μ XRD Investigation. *Appl. Phys. A Mater. Sci. Proc.* **2010**, *99*, 419–425. [[CrossRef](#)]

6. Meirer, F.; Liu, Y.; Pouyet, E.; Fayard, B.; Cotte, M.; Sanchez, C.; Andrews, J.C.; Mehta, A.; Sciau, P. Full-field XANES Analysis of Roman Ceramics to Estimate Firing Conditions: A Novel Probe to Study Hierarchical Heterogeneous Materials. *J. Anal. At. Spectrom.* **2013**, *28*, 1870–1883. [\[CrossRef\]](#)
7. Olivieri, L.M. The Last Phases at Barikot: Domestic Cults and Preliminary Chronology. Data from the 2012 Excavation Campaign in Swat. *J. Inner Asian Art Archaeol.* **2015**, *6*, 1–40. [\[CrossRef\]](#)
8. Olivieri, L.M. The Last Phases at Barikot: Urban Cults and Sacred Architecture. Data from the Spring 2013 Excavation Campaign in Swat. *J. Inner Asia Art Archaeol.* **2017**, *7*, 7–30. [\[CrossRef\]](#)
9. Olivieri, L.M. Physiology and meaning of pottery deposits in urban contexts (Barikot, Swat): Archaeological fieldnotes with an addendum on the *lāsana*/λάσανα pottery forms. *Ancient Pakistan* **2018**, in press.
10. Callieri, P.; Olivieri, L.M. *Ceramics from the Excavations in the Historic Settlement at Bīr-koṭ-ghwaṇḍai (Barikot), Swat, Pakistan (1984–1992)*, ACT-Field School Reports and Memoirs, Special Volume, 2; Sang-e-Meel Publications: Lahore, Pakistan, 2018; in press.
11. Allchin, F.R. Technical Description and Evaluation of the Pots and Potsherds. In *Ancient Buddhist Scrolls from Gandhāra. The British Library Kharoṣṭhī Fragments*; Salomon, R., Ed.; University of Washington Press: Seattle, WA, USA, 1999; pp. 183–187. ISBN 978-0295977690.
12. Whitbread, I.K. A proposal for the systematic description of thin sections towards the study of ancient ceramic technology. In *Archaeometry: Proceedings of the 25th International Symposium*; Maniatis, Y., Ed.; Elsevier: Amsterdam, The Netherlands, 1989; pp. 127–138.
13. Whitbread, I.K. *Greek Transport Amphorae—A Petrological and Archaeological Study*; Fitch Laboratory Occasional Paper; British School at Athens: Athina, Greece, 1995; Volume 4, ISBN 9780904887136.
14. Quinn, P.S. *Ceramic Petrography: The Interpretation of Archaeological Pottery & Related Artefacts in Thin-Sections*; Archaeopress: Oxford, UK, 2013; ISBN 978-1905739592.
15. Fauth, F.; Peral, I.; Popescu, C.; Knapp, M. The new Material Science Powder Diffraction beamline at ALBA Synchrotron. *Powder Diffr.* **2013**, *28*, S360–S370. [\[CrossRef\]](#)
16. Rius, J.; Labrador, A.; Crespi, A.; Frontera, C.; Vallcorba, O.; Melgarejo, J.C. Capabilities of through-the-substrate microdiffraction: Application of Patterson-function direct methods to synchrotron data from polished thin sections. *J. Synchrotron Radiat.* **2011**, *18*, 891–898. [\[CrossRef\]](#) [\[PubMed\]](#)
17. Rius, J.; Vallcorba, O.; Frontera, C.; Peral, I.; Crespi, A.; Miravittles, C. Application of synchrotron through-the-substrate microdiffraction to crystals in polished thin sections. *IUCr* **2015**, *2*, 452–463. [\[CrossRef\]](#) [\[PubMed\]](#)
18. Vallcorba, O.; Casas, L.; Colombo, F.; Frontera, C.; Rius, J. First terrestrial occurrence of the complex phosphate chladniite: Crystal-structure refinement by synchrotron through-the-substrate microdiffraction. *Eur. J. Mineral.* **2017**, *29*, 287–293. [\[CrossRef\]](#)
19. Maritan, L.; Nodari, L.; Mazzoli, C.; Milano, A.; Russo, U. Influence of firing conditions on ceramic products: Experimental study on clay rich in organic matter. *Appl. Clay Sci.* **2006**, *31*, 1–15. [\[CrossRef\]](#)
20. Gosselain, O.P. Bonfire of the enquiries: Pottery firing temperatures in archaeology: What for? *J. Archaeol. Sci.* **1992**, *19*, 243–259. [\[CrossRef\]](#)
21. Gualtieri, A.; Bellotto, M.; Artioli, G.; Clark, M. Kinetic study of the kaolinite mullite reaction sequence. Part I: Kaolinite dehydroxylation. *Phys. Chem. Miner.* **1995**, *22*, 207–214. [\[CrossRef\]](#)
22. Aras, A. The change of phase composition in kaolinite- and illite-rich clay-based ceramic bodies. *Appl. Clay Sci.* **2004**, *24*, 257–269. [\[CrossRef\]](#)
23. Nodari, L.; Marcuz, E.; Maritan, L.; Mazzoli, C.; Russo, U. Hematite nucleation and growth in the firing of carbonate-rich clay for pottery production. *J. Eur. Ceram. Soc.* **2007**, *27*, 4665–4673. [\[CrossRef\]](#)
24. Cultrone, G.; Sebastián, E.; Elert, K.; de la Torre, M.J.; Cazalla, O.; Rodriguez-Navarro, C. Influence of mineralogy and firing temperature in the porosity of bricks. *J. Eur. Ceram. Soc.* **2004**, *34*, 547–564. [\[CrossRef\]](#)
25. Faccenna, C.; Lorenzoni, S.; Olivieri, L.M.; Zanettin Lorenzoni, E. Geo-archaeology of the Swat valley (NWFP, Pakistan) in the Charbagh-Barikot Stretch: Primary note. *East West* **1993**, *41*, 1–4.
26. Bayley, S.W. X-ray diffraction identification on the polytypes of mica, serpentine and chlorite. *Clays Clay Miner.* **1988**, *36*, 193–213. [\[CrossRef\]](#)
27. Hey, M.H. A review of the chlorites. *Mineral. Mag.* **1954**, *30*, 277–292. [\[CrossRef\]](#)
28. Riccardi, M.P.; Messiga, B.; Duminuco, P. An approach to the dynamics of clay firing. *Appl. Clay Sci.* **1999**, *15*, 393–409. [\[CrossRef\]](#)

29. Ewel, R.H.; Bunting, E.N.; Geller, R.F. Thermal decomposition of talc. *J. Res. Natl. Bur. Stand.* **1935**, *15*, 551–556. [[CrossRef](#)]
30. Deer, W.A.; Howie, R.A.; Zussman, J. *Rock Forming Minerals*, 3rd ed.; Longman Scientific & Technical: New York, NY, USA, 2013; ISBN 978-0903056274.
31. Deldicque, D.; Rouzaud, J.N.; Velde, B. A Raman e HRTEM study of the carbonization of wood: A new Raman-based paleothermometer dedicated to archaeometry. *Carbon* **2016**, *102*, 319–329. [[CrossRef](#)]



© 2018 by the authors. Licensee MDPI, Basel, Switzerland. This article is an open access article distributed under the terms and conditions of the Creative Commons Attribution (CC BY) license (<http://creativecommons.org/licenses/by/4.0/>).